AIAA AVIATION Forum
June 25-29, 2018, Atlanta, Georgia
2018 Aerodynamic Measurement Technology and Ground Testing Conference

10.2514/6.2018-2989

Application of STARFLEET Velocimetry in the NASA Langley 0.3-meter Transonic Cryogenic Tunnel

Daniel Reese* and Paul Danehy†
Advanced Measurements and Data Systems, NASA Langley Research Center, Hampton, Virginia, 23681

Naibo Jiang‡, Josef Felver§, and Daniel Richardson**
Spectral Energies, LLC, Dayton, Ohio, 45430

and

James Gord††
Aerospace Systems Directorate, Air Force Research Laboratory, Wright-Patterson Air Force Base, Ohio, 45433

Selective two-photon absorptive resonance femtosecond laser electronic excitation tagging (STARFLEET) velocimetry is demonstrated for the first time in a NASA Langley wind tunnel with high repetition-rate and single-shot imaging. Experiments performed in the 0.3-meter Transonic Cryogenic Tunnel (TCT) allowed for testing at 300 K over a range of pressures (124 to 517 kPa) and Mach numbers (0.2-0.8) for freestream conditions and flow behind a cylindrical model. Measurement precision and accuracy are determined for the current set of experiments, as are signal intensity and lifetime. Precisions of 3-5 m/s (based on one standard deviation) were typical in the experiment; precisions better than 2% of the mean velocity were obtained for some of the highest velocity conditions. Agreement within a mean error of 3 m/s between STARFLEET freestream velocity measurements and facility DAS readings is demonstrated. STARFLEET is also shown to return spatially-resolved velocity profiles, though some binning of the signal is required.

Nomenclature

General Symbols

A	=	area [m^2]
C_p	=	specific heat, constant pressure [J/kg-K]
g	=	gravitational acceleration [m/s^2]
I	=	intensity [a.u.]
P	=	pressure [Pa, kPa]
t	=	time [s]
T	=	temperature [K]
u	=	velocity [m/s]

Greek Symbols

Δ	=	generic change
ε	=	generic error
ρ	=	density [kg/m^3]
σ	=	standard deviation or precision
τ	=	time constant [μs]

Subscripts and Superscripts

DAS	=	data acquisition system
i	=	spatial index(x,y,z)
j	=	frame index
RMS	=	root mean square
t	=	total or stagnation
w	=	wall
0	=	initial

* Research Engineer, National Institute of Aerospace, Hampton, VA, AIAA Young Professional Member
† Senior Technologist, AIAA Associate Fellow
‡ Research Scientist, AIAA Associate Fellow
§ Research Scientist, AIAA Member
** Research Scientist, AIAA Member
†† Principal Research Chemist, AIAA Fellow

I. Introduction

GROUND-TESTING at flight-accurate Reynolds numbers is imperative for the continued safety and success of flight vehicle research and development. Transonic cryogenic tunnels (TCTs) such as the National Transonic Facility (NTF) at The NASA Langley Research Center allow testing in this regime, as they have been shown to reach Reynolds numbers exceeding 4×10^8 m^{-1}.[1] This is achieved by injecting cold nitrogen into the flow, which reduces the viscosity and increases the density of the flow by creating a high-pressure, low-temperature environment. While operating under these conditions produces flight-accurate Reynolds numbers, it demands sturdy construction of the facility (and any hardware needed for measurements) in order to withstand the high pressures and thermal stresses present during testing. This often leads to extremely limited optical access to the test section, making many measurement techniques difficult — or impossible — to carry out in TCTs. In addition to these physical limitations, organizational and facility regulations can often impede the use of certain measurement techniques. In some TCTs, techniques such as particle image velocimetry (PIV) and Doppler global velocimetry (DGV) are disallowed due to their dependence on tracer particles being introduced into the flow, since these tracer particles can damage sensitive facility components or condense on test models causing surface roughness. As such, diagnostics are traditionally limited to integrated force and moment measurements, or other on-body measurements through the use of pressure- and temperature-sensitive paint. Off-body measurements in TCTs remain limited mainly to probes although a few laser based techniques have been used in TCTs as recently reviewed by Burns et al.[2,3,4,5,6]

One class of diagnostics that has proven effective in producing off-body velocity measurements in TCTs is molecular tagging velocimetry (MTV). MTV techniques such as femtosecond laser electronic excitation tagging (FLEET) and picosecond laser electronic excitation tagging (PLEET) do not require the addition of tracer particles and have been successfully employed in the NASA Langley 0.3-m TCT. FLEET and PLEET velocimetry work by focusing an ultrafast laser pulse to directly excite and dissociate molecular nitrogen (N_2); upon recombination of the nitrogen atoms, light is emitted and can be tracked over two or more frames to provide an estimate of the local flow velocity and potentially acceleration. While these methods lend themselves to use in TCTs due to their ability to provide unseeded velocity measurements in N_2, both techniques have physical limitations that must be considered. Perhaps the most important factor to consider with these MTV techniques is the large thermal perturbation resulting from the excitation process.[7,8,9] Furthermore, the high laser powers used can potentially damage wind tunnel windows and models. These drawbacks of FLEET and PLEET can be mitigated using selective two-photon absorptive resonance FLEET (STARFLEET).[8]

STARFLEET is an additional member of the MTV class of velocimetry techniques, and uses a 202.25 nm femtosecond laser to resonantly excite nitrogen.[8] The technique has been previously demonstrated in a laboratory-scale jet flow using low speed cameras and multi-shot accumulations.[8] By frequency-quadrupling an 809 nm laser (a similar wavelength as typically used for non-resonant FLEET), the overall amount of energy required to excite the nitrogen is reduced by about a factor of 30,[8] thus drastically decreasing the thermal perturbation introduced by the measurement technique. Unfortunately, the advantage of reduced energy input from the laser system is not without its downsides. The deep UV wavelengths required for optimized excitation makes transmitting the laser beam over long distances difficult, and necessitates the use of special windows and optics. In this study, magnesium fluoride (MgF_2) windows and lenses were required to allow passage of the laser light into the wind tunnel test section and to write the STARFLEET line.

The experimental campaign described within this manuscript constitutes the first application of STARFLEET velocimetry in a wind tunnel, and also the first application of high-speed, single-shot STARFLEET. Data was obtained and analyzed for freestream conditions at 300 K covering 9 flow conditions, including pressures from 124-517 kPa (18-75 psi) and Mach numbers from 0.2-0.8. This paper continues with a description of the experimental setup in section II, while section III discusses the data processing. Results such as freestream velocity measurements, as well as precision and accuracy estimates are presented in Section IV, and final conclusions are drawn in Section V.

II. Experimental Setup

Experiments were conducted in the NASA Langley 0.3-m TCT; a closed-loop, fan-driven, cryogenic wind tunnel. Although capable of running with several different test gases, only nitrogen was used in the present studies for the ability to obtain the highest Reynolds numbers and for optimal performance of STARFLEET. The facility has a 0.33 m × 0.33 m test section surrounded by a pressurized plenum, and is capable of stably operating at total pressures ranging from 124 to 517 kPa, total temperatures from 100 to 325 K, and Mach numbers from 0.2 to 0.85. An array of wall pressure taps, thermocouples, pitot probes, pressure transducers, and strain gauges make up the facility data acquisition system (DAS), and DAS instrument readings were used as a basis of comparison for results obtained from

STARFLEET measurements. Fused silica (SiO_2) windows in the test section and outer plenum provided optical access for the camera, while MgF_2 windows allowed for laser penetration into the test section. A schematic showing the experimental setup, including a layout of the camera, laser path, optics, plenum, and test section is shown in Fig. 1.

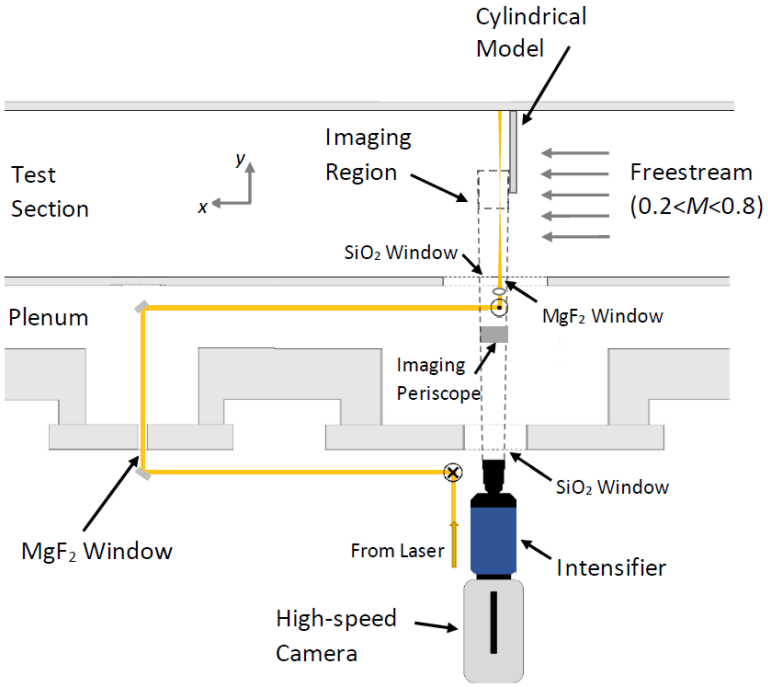

Figure 1. Schematic of the experimental setup as seen from above.

A regeneratively-amplified Ti:Sapphire laser system (Spectra-Physics Solstice) with a repetition rate of 1 kHz, center wavelength of 809 nm, and bandwidth of 13 nm was used as input to a frequency-quadrupler in order to create the 202.25 nm light that was used to write the STARFLEET line. Although the laser system produced approximately 60 µJ per pulse at the exit of the quadrupler, only 8 µJ per pulse was present inside of the test section. This large drop in power was caused by the combined effect of absorption of the UV laser propagating through air, as well as additional losses incurred at each mirror (typically with 85% reflectivity) and window (~92% transmission). Prior to passing through the test section MgF_2 window, the laser beam was focused using a 250 mm MgF_2 spherical lens in order to write the STARFLEET line.

STARFLEET signal was recorded using a UV high-speed image intensifier (LaVision HS-IRO with an S20 photocathode) lens-coupled to a high-speed CMOS camera (Photron SA-Z). Imaging was done through a 100-mm, *f*/2 UV Halle lens yielding a magnification of approximately 160 µm/px. For each run condition, four frames of data (with 1 µs exposure every 2.5 µs, corresponding to a rate of 400 kHz) are captured for ~20,000 sets of data. While each set contains four frames of data, there is only one laser pulse per set. A total of 9 conditions were investigated by changing the flow pressure (P=124, 276, and 517 kPa) and Mach number (M=0.2, 0.5, and 0.8). Velocity measurements were made in freestream conditions, as well as for the case of flow behind a 1" cylindrical model. The processing of raw data obtained in these studies is discussed further in the following section.

III. Data Analysis

Discussed in detail within this section are the various processing steps needed to obtain STARFLEET signal and velocimetry results. Subsection A outlines the preprocessing stage, which includes the dewarping, scaling and binning of data. Subsection B covers the methods used to determine the peak signal location to sub-pixel accuracy from the preprocessed STARFLEET image sets. Finally, subsection C contains an analysis of the displacement calculations to obtain spatially-resolved velocity measurements.

A. Preprocessing (Signal Dewarping, Scaling, and Binning)

There are more than 20,000 sets of data (20,000 individual single-shot velocity measurements) for each of the 9 conditions covered in these experiments, and every set contains 4 frames of STARFLEET signal plus background images. The first step in the preprocessing stage is to apply an image dewarping to correct every frame for lens effects and perspective distortion resulting from the oblique camera viewing angle. This is achieved by taking a set of calibration images of a target placed such that the target face is parallel to the path of the laser in the imaging plane. This is the same method used in many similar MTV experiments, though different than prior FLEET and PLEET experiments in the 0.3 meter TCT where the target was placed normal to the laser beam.[2,7] The target used in the present work consisted of a regular grid pattern of small dots, with 6.2 mm spacing between points. Dot locations in the calibration images are determined using a custom centroid-finding algorithm, and each point is then mapped to

the expected location given the known target pattern. The calculated transformation is then applied to all frames of STARFLEET data. Since the physical spacing between target dot centroids is known, this method of data dewarping also allows for the extraction of a scale factor used to bring the STARFLEET signal data from pixel spacing into physical units. Sample dewarped STARFLEET images (in physical units) can be seen along the top row of Fig. 2, where the leftmost image is the first frame of data, and each succeeding image is the following frame within the set. In this figure, the STARFLEET line is shown as a dark, vertical line which first appears just to the left of x=3.2 mm, but shifts rightward as it tracks the flow with each subsequent frame.

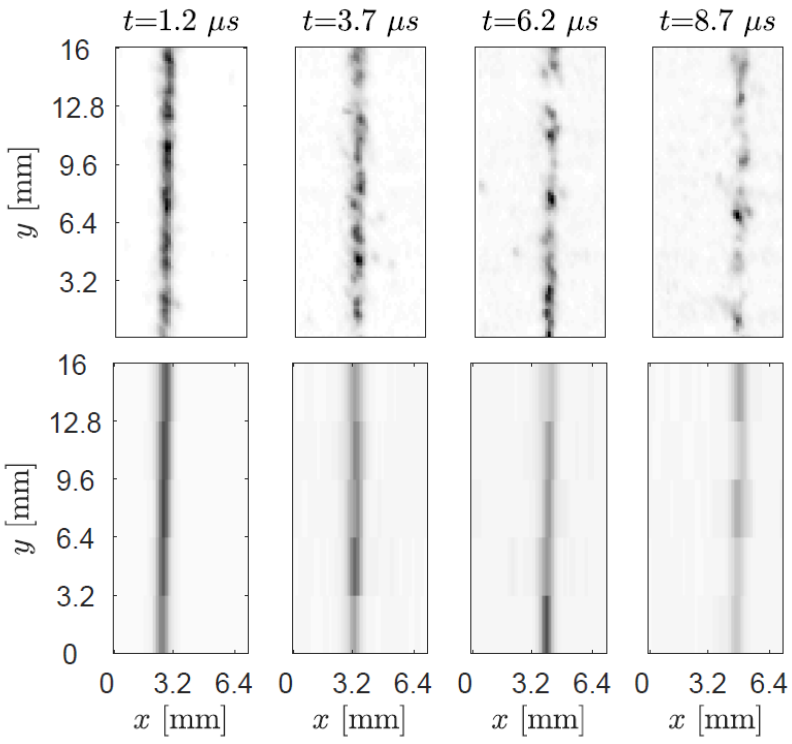

Figure 2. Raw vs. binned STARFLEET signal. Top row shows raw STARFLEET signal for each of four frames; bottom row shows the corresponding data binned to 5 rows for each frame.

Earlier work using similar MTV techniques in the 0.3-meter TCT have almost exclusively utilized boresight (or near-boresight) configurations wherein the camera's view of the signal is along or nearly along the laser's path.[10,11] These studies have traditionally relied on imaging signal from an integrated region along the excited line to obtain the signal-to-noise ratio (SNR) necessary to make accurate and precise single-point, two-component velocity measurements. In the present work however, an imaging geometry where the laser is directed into the flow through one window and the camera images through another window (parallel to the first) allows for spatially-resolved velocity measurements in the y direction. Several factors led to the use of this geometry in addition to the desire for spatial resolution. First the STARFLEET signal appears to be much longer (on the order of 20-30 mm) compared to FLEET or PLEET (which produce ~2 mm long signal regions) while using similar focusing lenses. Using a boresight-type configuration with STARFLEET would therefore result in an order of magnitude larger spatial averaging. Also, MgF_2 windows had to be used for the laser beams and these windows are relatively expensive, so small windows were used that were too small for the camera to image the signal. Consequently, the use of this geometry results in decreased SNR compared to the prior FLEET and PLEET experiments in this facility. The SNR in the boresight configuration is higher than non-boresight because in the boresight configuration all of the emission is spatially integrated on a small spot on the detector. In the current experiment, this light is spread out into a line over multiple pixels. This compromised SNR, in addition to the already-low pumping energy used to write the STARFLEET line, requires the use of binning to obtain results comparable to those found in previous studies. The effect of bin size on the precision of velocity measurements was investigated, and served as the principal

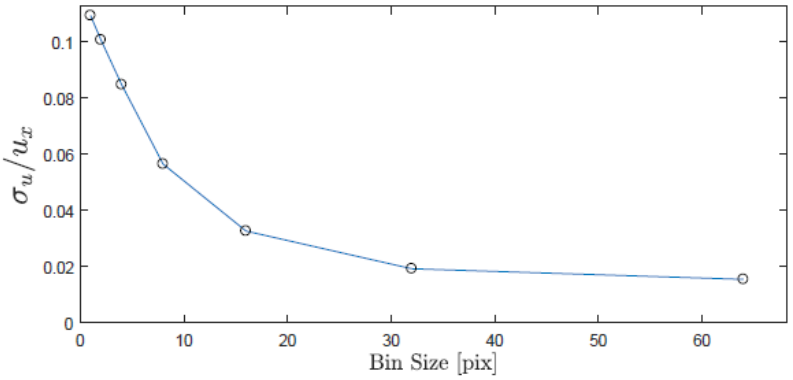

Figure 3. Precision measurements (as a percentage of the mean velocity) as a function of bin size. A final bin size of 20 was chosen for data analysis, allowing for more precise, spatially-resolved velocity estimates.

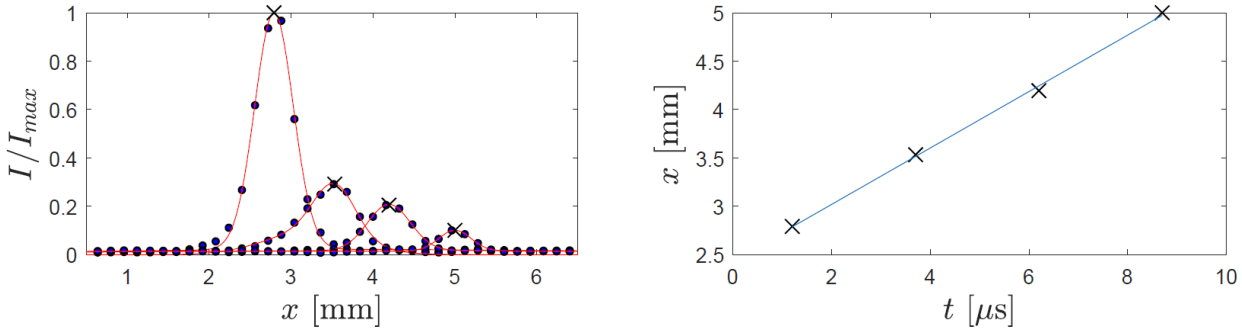

(a) *(b)*

Figure 4. Binned, single-shot signal intensity (normalized by the maximum intensity) for each of four frames of data is shown in (a) as black dots; the corresponding fits are shown as red lines, with peak intensities/locations marked with black 'x'. Peak signal locations are plotted as a function of time in (b), where the slope of the blue fit line gives an estimate of velocity.

metric used to determine the bin size for further analysis. Figure 3 shows the effect of varying bin size on the standard deviation of velocity measurements for the M=0.8, P=517 kPa case. A bin size of 20 pixels was ultimately chosen, as this yielded nearly as good precision (2-3%) and spatial resolution (~3 mm) to previous studies[9,10] while allowing for the extraction of velocity from five y locations spanning the wind tunnel test section. It is this binned STARFLEET signal that is used in the analysis that follows. Representative binned STARFLEET signal images are shown along the bottom row of Fig. 2.

B. Determination of Peak Signal Location

The next step of analysis entails determining the x location of the peak signal intensity for all y locations and frames within each set. The following two-term Gaussian model is fit to the preprocessed STARFLEET data in order to determine the peak signal location with sub-pixel accuracy,

$$G_2(x) = a_1 \exp\left[-\left(\frac{x-b_1}{c_1}\right)^2\right] + a_2 \exp\left[-\left(\frac{x-b_2}{c_2}\right)^2\right], \quad (1)$$

where the first Gaussian term is fit to the background signal, ensuring that the second term of $G_2(x)$ provides a proper fit to the STARFLEET signal. From this fit, an x location corresponding to the peak signal intensity is extracted to sub-pixel accuracy for each y location and frame. Figure 4a shows results from all four frames of data for a single y location of STARFLEET signal. The intensity (normalized by the maximum intensity of the set) for all four frames are shown as black points, and red lines indicate the corresponding fit of each frame. At the peak of each fit, a black 'x' indicates the measured location of the peak STARFLEET signal. Once the peak signal location has been determined for all y locations and frames within a set, this position information can be used to determine velocity using a number of different velocity estimation schemes. Details on the method chosen for use in the present work are provided in the following subsection.

C. Velocity Calculations

Because more than two frames of STARFLEET signal were obtained in the current study, there are several ways to extract velocity estimates once peak signal locations have been determined. Burns et al. conducted a study of various schemes (including point-to-point, linear regression, and polynomial fitting) and showed that the linear regression method exhibited the highest measure of accuracy and precision.[7,10,11] In this work, a similar linear fit to peak signal location in time is performed to calculate flow velocity, with several constraints introduced to ensure that only valid and physical velocity results are considered.

The first restriction applied to the data was that only locations determined from intensities above a certain threshold were included in the velocity fit; since the background signal is nominally constant throughout this set of experiments, this condition ensures that frames with low SNR are rejected. This restriction eliminated about 3.5% of the frames. Next, the fit was required to pass through the first peak signal location, even if a better R^2-value could have been attained by allowing the fit to intercept the position axis at a location different than that of the initial point. Finally, all velocity fits with R^2<0.97 were excluded from consideration. This restriction eliminated a further 2% of the data. A

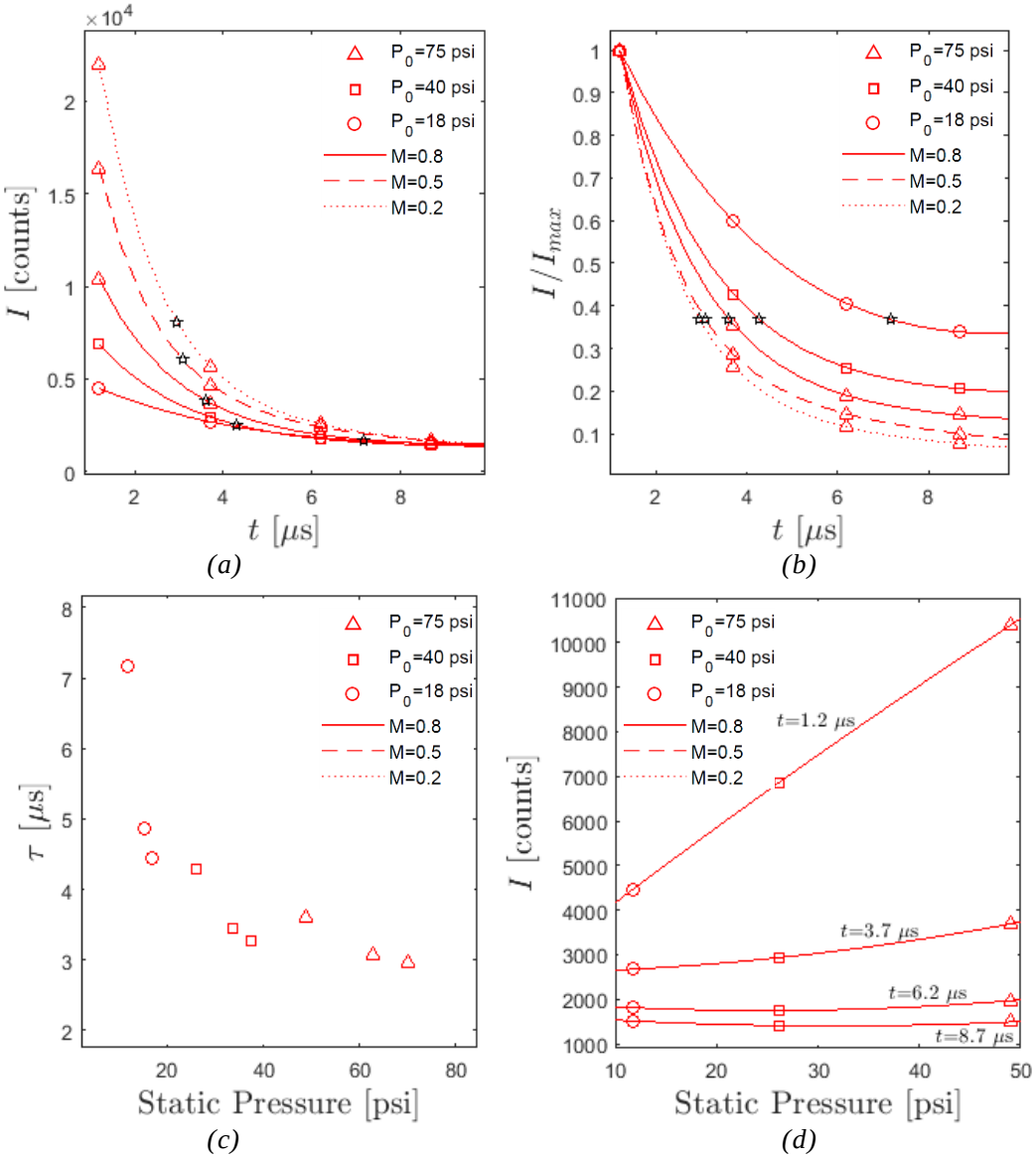

Figure 5. Signal intensity and lifetime measurements. (a) Absolute intensity measurements as a function of time for various pressures and Mach numbers; black stars indicate the signal lifetimes for each case. (b) Normalized intensity measurements showing the largest intensity values give the most rapid signal decay. (c) Lifetime measurements as a function of static pressure indicating higher pressures correspond to shorter lifetimes. (d) Intensity as a function of static pressure for all four frames of data from the *M*=0.8 case.

typical linear fit to peak signal location in time is shown in Fig. 4b. Each peak signal location determined by the method described in subsection B (and shown as a black 'x' in Fig. 4a) is shown as a black 'x' in Fig. 4b, while the fit to this data is shown as a solid blue line. The velocity for this set of data is determined by the slope of the fit line.

IV. Results and Discussion

This section highlights the STARFLEET results obtained from experiments in the 0.3-m TCT. Subsection A covers signal intensity and lifetime measurements of the STARFLEET signal over a range of tunnel operating conditions. Velocity measurements, including profiles and comparison with facility values, are displayed and discussed in subsection B. Lastly, the precision and accuracy of velocity results are studied in subsection C.

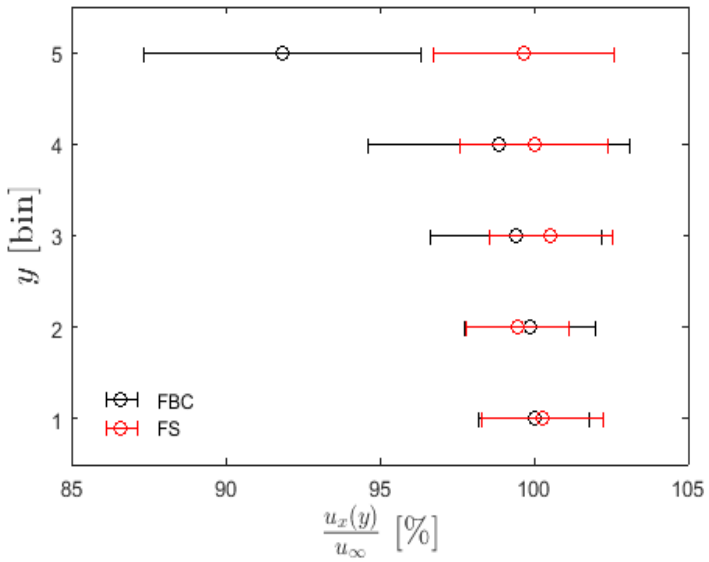

Figure 6. Velocity profiles for the freestream (FS, red) and flow behind a cylindrical model (FBC, black). Error bars indicate the uncertainty in the mean.

A. Signal Intensity and Lifetime Measurements

Using the peak signal intensity for each *y* location and frame determined as in section III.B, the sensitivity of the STARFLEET signal to flow pressure and Mach number can be investigated. The effect of varying pressure and Mach number on signal intensity and lifetime is shown in Fig. 5a, where symbols differentiate flow pressures and line types indicate various Mach numbers. The three solid line fits to data of constant Mach number (M=0.8) reveal that the STARFLEET signal increases with increasing pressure. The effect of Mach number is also demonstrated in Fig. 5a (with M=0.2, 0.5, and 0.8 indicated by the dotted, dashed and solid lines, respectively), and shows a reduction in the measured peak intensities with increasing Mach number, for a given total pressure, P_0. This observation can be explained by the reduced static pressure owing to higher Mach, since the STARFLEET signal intensity is shown to decrease with a reduction of static pressure. The same data is shown normalized to the first frame in Fig. 5b, which more clearly shows that different conditions result in different lifetimes. Signal lifetime is shown as a function of static pressure for the high Mach case in Fig. 5c. Residual discrepancy may be attributed to the different static temperatures at different Mach numbers. Signal intensity is shown as a function of static pressure for the high Mach case in Fig. 5d.

In addition to providing insight into the sensitivity of the signal to flow conditions, intensity measurements can also be used to determine the STARFLEET signal lifetime which has important implications for making high-precision measurements. As conducted in similar MTV experiments,[11] signal intensity decay is fit as a function of time using a bi-exponential model,

$$I(t) = ae^{bt} + ce^{dt}. \tag{2}$$

The signal lifetime can then be defined to be the time that the signal reaches 1/e of the initial value. Intensity measurements and fits can be seen in Fig. 5a and 5b, where the red symbols show measured intensities, the red lines are the bi-exponential fits, and the black stars indicate the signal lifetimes for each case. The signal intensity lifetime measurements are also shown as a function of static pressure in Fig. 5c. The data suggest that static pressure has a significant effect on the lifetime with increasing pressures decreasing the lifetimes in agreement with the FLEET technique.[11] Static temperature varied less than 15% over the range of conditions in this plot.

B. Velocity Measurements

Velocity profiles were calculated for each set and all freestream conditions. Figure 6 shows a typical velocity profile from a single set for the M=0.8, P=517 kPa case, with the measured velocity at each *y* position as a percentage of the freestream velocity. Figure 6 shows profiles for both the freestream case and for flow behind a

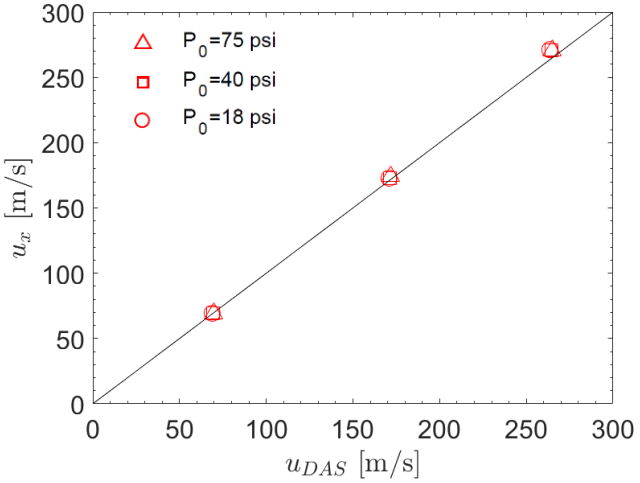

Figure 7. STARFLEET velocity measurements compared with facility DAS readings. Error bars are present but hidden by the data points. The solid line indicates perfect agreement.

cylinder, and the error bars indicate the uncertainty in the mean at each *y* location. As demonstrated in Fig. 6, the freestream profile shows nearly-constant velocity across the tunnel test section, while the profile corresponding to the case of flow behind a cylinder indicates a velocity deficit in the region behind the model.

In addition to spatially-resolved measurements, freestream velocity profiles (such as the one shown in Fig. 6) were collapsed to a single value for each set by averaging the velocities from each of the five *y* locations; all 20,000+ sets were then averaged to yield a single mean velocity measurement for each run condition and an uncertainty in that mean. Velocity measurements for all 9 cases considered in this study are summarized in Fig. 7, where they are compared against facility DAS measurements. No uncertainty error bars are seen because they are smaller than the size of the symbols used. A more detailed analysis of the precision and accuracy of STARFLEET velocity measurements is carried out in the following section.

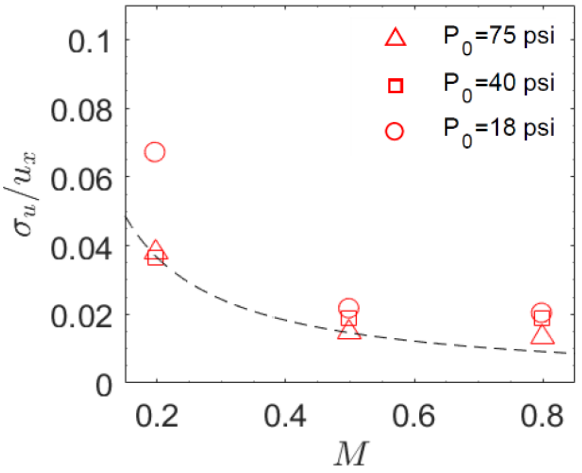

Figure 8. Precision (as a fraction of the mean freestream velocity) as a function of stagnation pressure and Mach number.

C. Measurement Precision and Accuracy

Accuracy measurements are made by comparison to the facility DAS values of velocity, and results are summarized in Fig. 7 for all 9 conditions covered in the present work. While the measured STARFLEET velocities generally tend to agree well with those reported by the facility DAS, the discrepancy appears to grow larger with increasing velocity. The maximum error between STARFLEET and DAS measured mean velocities was 7.7 m/s (corresponding to 2.9% of the freestream velocity) while the mean error was 3 m/s. This discrepancy could be partly caused by an error in calibration.

One standard deviation of the velocity measurements is taken to be the precision, which is shown as a fraction of the measured velocity in Fig. 8. Precision as a percentage of the mean velocity is shown to generally decrease with increasing Mach number, and to decrease with increasing pressure. The dashed line in this figure represents the trend of the optimal precision across all Mach numbers. Precisions better than 2% of the mean velocity were obtained for some conditions. While nearly all precision measurements lie below four percent of the freestream velocity, the worst-case precision measurement is near seven percent, owing, in part, to a low mean velocity in the denominator. These single-shot precision measurements correspond to a roughly constant value of 3-5 m/s, with the percent-precision decreasing for higher freestream velocities due to the larger denominator. In general, these precision measurements are an order of magnitude larger than results from similar MTV measurements made in the 0.3-m TCT.[10]

V. Conclusion

For the first time, high repetition-rate and single-shot STARFLEET velocimetry has been successfully demonstrated in a wind tunnel. The NASA Langley 0.3-m Transonic Cryogenic Tunnel allowed for flow measurements at 300 K over a wide range of Mach numbers and pressures. Signal intensity and lifetime dependence on these conditions was explored, and a reduction in intensity was shown for both increasing Mach number and decreasing pressure. Precision and accuracy of freestream velocity measurements was also explored. Precision was shown to generally be 3-5 m/s, which was typically 2-4% of the freestream value, and agreement within a mean error of 3 m/s between STARFLEET velocity measurements and facility DAS readings was demonstrated. Spatially-resolved velocity profiles were obtained for both the freestream and the flow behind a cylindrical model, and the STARFLEET method was shown to be sufficiently sensitive to measure the velocity deficit in the region behind the model.

Acknowledgments

The authors wish to thank Sukesh Roy, Spectral Energies, LLC for his support and leadership during this project. Also we thank the staff at the 0.3-meter TCT for their support, including: Wes Goodman, Mike Chambers, Cliff Obara, Tammy Price, Karl Maddox, and Reggie Brown. This work was supported by a NASA Langley IRAD Project and

NASA's Aerosciences Evaluation and Test Capabilities (AETC) Portfolio as well as a NASA SBIR NNX14CL74P, NNX15CL24C and Air Force Office of Scientific Research award Nos. 15RQCOR202 and 14RQ06COR.

References

[1] *National Transonic Facility: USER GUIDE*. National Aeronautics and Space Administration.

[2] Burns, R. A., and Danehy, P. M., "Unseeded Velocity Measurements Around a Transonic Airfoil Using Femtosecond Laser Tagging," *AIAA Journal*, Vol. 55, No. 12, (2017), pp. 4142-4154.

[3] Quest, J., and Konrath, R., "Accepting a Challenge—The Development of PIV for Application in Pressurized Cryogenic Wind Tunnels," *41st AIAA Fluid Dynamics Conference and Exhibit*, AIAA Paper 2011-3726, 2011.

[4] Willert, C., Stockhausen, G., Beversdorff, M., Klinner, J., Lempereur, C., Barricau, P., Quest, J., and Jansen, U., "Application of Doppler Global Velocimetry in Cryogenic Wind Tunnels," *Experiments in Fluids*, Vol. 39, No. 2, 2005, pp. 420–430.

[5] Gartrell, L. R., Gooderum, P. B., Hunter, W. W., and Meyers, J. F., "Laser Velocimetry Technique Applied to the Langley 0.3-Meter Transonic Cryogenic Tunnel," NASA TM-81913, 1981.

[6] Honaker, W. C., and Lawing, P. L., "Measurements in the Flow Field of a Cylinder with a Laser Transit Anemometer and a Drag Rake in the Langley 0.3-m Transonic Cryogenic Tunnel," NASA TM-86399, 1985.

[7] Burns, R. A. and Danehy, P. M., "FLEET Velocimetry Measurements on a Transonic Airfoil," *55th AIAA Aerospace Sciences Meeting*, Grapevine, TX, 2017, AIAA-2017-0026.

[8] Jiang, N., Halls, B. R., Stauffer, H. U., Danehy, P. M., Gord, J. R., and Roy, S., "Selective two-photon absorptive resonance femtosecond laser electronic excitation tagging velocimetry," *Optics Letters*, Vol. 41, No. 10, 2016, pp.2225-2228.

[9] Limbach, C. M., and Miles, R. B., "Rayleigh Scattering Measurements of Heating and Gas Perturbations Accompanying Femtosecond Laser Tagging," *AIAA Journal*, Pre-Print, 2016.

[10] Burns, R. A., Danehy, P. M., Halls, B. R., Jiang, N., "Application of FLEET Velocimetry in the NASA Langley 0.3-meter Transonic Cryogenic Tunnel," *31st AIAA Aerodynamic Measurement Technology and Ground Testing Conference*, Dallas, TX, 2015, AIAA-2015-2566.

[11] Burns, R. A., Danehy, P. M., Peters, C. J., "Multiparameter Flowfield Measurements in High-Pressure, Cryogenic Environments Using Femtosecond Lasers," *32nd AIAA Aerodynamic Measurement Technology and Ground Testing Conference*, Washington, D.C., 2016, AIAA-2016-3246.